IEEE Access
Multidisciplinary | Rapid Review | Open Access Journal

Received July 23, 2019, accepted July 27, 2019, date of publication July 31, 2019, date of current version August 15, 2019.

Digital Object Identifier 10.1109/ACCESS.2019.2932194

Identification of Coherent Generators by Support Vector Clustering With an Embedding Strategy

MEHDI BABAEI[1], (Member, IEEE), S. M. MUYEEN[1], (Senior Member, IEEE), AND SYED ISLAM[2], (Fellow, IEEE)

[1]School of Electrical Engineering, Computing and Mathematical Sciences, Curtin University, Perth, WA 6102, Australia
[2]School of Science, Engineering and Information Technology, Federation University, Ballarat, VIC 3353, Australia

Corresponding author: Mehdi Babaei (mehdi.babaei@postgrad.curtin.edu.au)

This work was supported in part by the Australian Government Research Training Program Scholarship, and in part by the Curtin University Postgraduate Scholarship.

ABSTRACT Identification of coherent generators (CGs) is necessary for the area-based monitoring and protection system of a wide area power system. Synchrophasor has enabled smarter monitoring and control measures to be devised; hence, measurement-based methodologies can be implemented in online applications to identify the CGs. This paper presents a new framework for coherency identification that is based on the dynamic coupling of generators. A distance matrix that contains the dissimilarity indices between any pair of generators is constructed from the pairwise dynamic coupling of generators after the post-disturbance data are obtained by phasor measurement units (PMUs). The dataset is embedded in Euclidean space to produce a new dataset with a metric distance between the points, and then the support vector clustering (SVC) technique is applied to the embedded dataset to identify the final clusters of generators. Unlike other clustering methods that need a priori knowledge about the number of clusters or the parameters of clustering, this information is set in an automatic search procedure that results in the optimal number of clusters. The algorithm is verified by time-domain simulations of defined scenarios in 39 bus and 118 bus test systems. Finally, the clustering result of 39 bus systems is validated by cluster validity measures, and a comparative study investigates the efficacy of the proposed algorithm to cluster the generators with an optimal number of clusters and also its computational efficiency compared with other clustering methods.

INDEX TERMS Coherent generators, dynamic coupling, embedding, slow coherency, support vector clustering, synchrophasor.

I. INTRODUCTION

Despite all the efforts have been devoted to group the generators in certain coherent groups according to their similar oscillatory behavior after a disturbance, the traditional offline coherency studies are not able to fully demonstrate the dynamic behavior of power systems [1]. On the other hand, the gradual increase of demand in the electricity market makes the power system operate at a point closer to its stability margins, and the power system is more vulnerable to the complicated dynamic behavior of the system following a disturbance [2]. Furthermore, the impact of renewable power generation on interarea oscillations of power system shows that a power system with a high penetration level of renewable generation can be pushed toward the unstable zone of operation at certain oscillation modes [3]–[5]. Therefore, conventional model-based monitoring and control systems, which are designed for a specific operating condition, are not robust enough to track all dynamical responses of power system caused by the heterogeneous dynamic behavior of inverter connected renewable energy sources. Under such conditions, developing a suitable data-based monitoring system in a wide area power network, which depend on collected measurements in online applications, is more desirable to detect the transient oscillations between different areas. This can be achieved with the assistance of Synchrophasor technology, i.e., deployment of PMUs at appropriate buses and design a reliable wide area monitoring, protection, and control (WAMPC) system to secure the stable operation and avoid a widespread blackout [6]. If local protective systems fail to detect and operate against power system disturbances, WAMPC system becomes active as the second line of defence. The continuous surveillance of oscillations between the emerged CGs in the post-disturbance condition is the primary duty of such a WAMPC system. In this context, generator coherency refers to the natural tendency of

The associate editor coordinating the review of this manuscript and approving it for publication was Md. Shihanur Rahman.

a group of generators in a power system swinging together against other groups of generators after the occurrence of a disturbance [7]. The motivation for improving the generator coherency studies comes from the necessity of applying the results of coherency analysis to some applications of WAMPC system such as controlled islanding to split the power system into a distinct number of self-sustaining islands [8], and Wide-area Control [9] or other applications such as power system model reduction [10]. The interarea oscillation modes and emergence of coherent areas are mainly recognized by some intrinsic characteristics of the grid such as the number of internal and external lines of each area and the impedance of interconnection lines [10]; however, protective schemes cannot rely only on offline studies due to the unpredictable behavior of some loosely coherent generators in each area [11]. Therefore, online identification of CGs is inevitable.

Generally, there are two approaches to the study of generator coherency [12]. The model-based approach is used in slow coherency based studies [7], [8], [10] in which the oscillation modes are extracted from the Eigenanalysis of a small-signal model of power system [7]. In some early works, the validity of using a simplified linear model of power system for coherency analysis even in large disturbance conditions was demonstrated in [13]. Applying the singular perturbation theory to two-time-scale power system model [7], [14] shows that there is a connection between slow coherency and weak connections in power systems. Slow coherency solves the problem of CG identification by finding weak connections between the CGs. In this approach, the coherency of generators is not affected by the location and severity of disturbances in the power system [8]; however, it is sensitive to the changes in system operating conditions. A method was devised in [15] to trace the eigenvalues of the system to update the CGs after any change in system condition caused by disturbances. Effectiveness of applying the model-based slow coherency to find the proper cutsets of controlled islanding schemes in a very large power system such as Western Electricity Coordinating Council (WECC) system in North America with 15000 buses was investigated in [16].

The measurement-based approach is implemented extensively in contingency studies using time domain simulation of different scenarios to analyze the dynamic response of generators and is independent of the detailed model of the power system. The motivation behind some studies was to use PMU measurements to construct a reduced-order model of large power system and capture the slow oscillation between coherent areas or even transient stability margins due to disturbances. Although a reduced-order model of the power system is constructed in these studies, they should not be confused with small signal model based methods. The aggregated models of the WECC network obtained in [17], [18] captured the dynamic response of the network to different disturbances, however, it is not possible to trace the dynamic behavior of each generator in a five-machine model of WECC system. Other measurement-based coherency studies are based on a coherency criterion as the basis of splitting the generators, such as the frequency response of rotor angles [19], frequency deviation of terminal buses of generators with respect to system nominal frequency [20], and the difference between phases of dominant modes in the frequency spectrum of rotor speed deviations [21]. Statistical assessment tools such as signal correlation coefficients and Spearman's rank correlation coefficients were used in some other studies [2], [22], [23] for assessing the correlation between angle and speed signals of generator pairs. In [24], a method based on the wavelet transform of the phase difference of generator rotor angles was proposed. Modal analysis of swing curves was performed by Koopman operator in [25] to extract the Koopman modes and recognize the coherent generators. The phase of oscillation modes was considered as coherency criterion in [26] by implementing Empirical Mode Decomposition (EMD) technique combined with Hilbert transform. A new multiflock-based coherency identification was introduced in [27] that was inspired by the flocking behavior of nature.

In contrast, some other studies employ clustering techniques to separate the CGs based on an appropriate predefined distance measure in Euclidean space. K-means clustering technique combined with a competitive neural network algorithm was proposed in [28] based on a speed criterion as the coherency measure. Fuzzy C-means (FCM) clustering was applied in [29]. Since FCM clustering method needs random initialization and is time-consuming in large power systems, another improved FCM clustering method (FCMdd) was suggested in [12], [30] to tackle these problems by an offline probabilistic coherency analysis of generators. Also, subtractive clustering was proposed in [31] to overcome the limitation of such dependence on random initialization. The first three principal components of generator speed and bus angles were obtained and then clustered by using Principal Component Analysis (PCA) technique in [32]. The idea of extracting the principal components of rotor angles was extended in [33] by using a statistical technique to find the optimal direction in projection from multi-dimensional to low dimensional space. Spectral clustering algorithm has also shown its effectiveness regarding simplicity, readiness and its capability to define user-defined similarities [1]. A new data-driven similarity measure was extracted in [34] by combining several similarity indices based on generator rotor angle and rotor speed trajectories and then spectral clustering was applied to obtain the CGs. A similar approach with multiple similarity indices was adopted in [22] to derive the similarity index, but agglomerative hierarchical clustering was applied instead, to separate the generators. Hierarchical clustering was also used in [35], [36] to motion trajectories of power system based on similarity matrix and pattern recognition techniques respectively. Kernel Principal Component Analysis (KPCA) method was employed in [37] to reduce the dimension of data and integrate multiple similarity indices into a data-driven coherency detection algorithm,

then Affinity Propagation (AP) method was accomplished to cluster the generators, but only rotor angle and rotor speed were considered for computing the similarity indices. Support vector clustering was also applied before [38] directly on angle or speed deviation of generators; however, it was shown in [21] that the rotor angle deviation could result in the wrong grouping of generators. This study, which employed the concept of slow coherency of generators in a measurement-based coherency detection method, also indicates that the dynamic coupling is a more reliable coherency measure than angle or speed deviation of generators.

All generator coherency studies are necessarily built on two fundamental bases: a coherency measure and a technique to separate the generators according to the coherency measure. This study proposes the dynamic coupling between the generators as the coherency measure along with applying SVC technique on embedded data points to determine the CGs. All referred clustering-based methods are dependent on a priori knowledge about the number of clusters [39] or have some shortcomings such as recursive separation as seen in [11] and [40]. To overcome these limitations, an online coherency identification method is introduced in this study that not only results in the formation of CGs with more reliable coherency measure but also is independent of a predefined number of clusters and can automatically set the parameters of the clustering procedure such that the optimal clustering structure is obtained. Furthermore, by applying the SVC technique, any clustering algorithm is benefitted from the merits of finding the clusters of a dataset with arbitrary shaped boundaries, which is the unique advantage of the SVC [41]. Another interesting aspect of the present work is incorporating an embedding strategy in the clustering algorithm to apply the clustering technique on a dataset with an inherent Non-Euclidean distance measure.

Therefore, the contributions of this work include: 1) proposing an online coherency detection method that is independent of a priory knowledge of number of partitions 2) adopting an embedding strategy in coherency identification algorithm to incorporate any Non-Euclidean distance measure in clustering procedure. In order to present the framework, first, the coherency criterion is introduced in section II, then after reviewing the background of support vector clustering in section III, the required steps of preprocessing the input data to be prepared for the clustering algorithm are explained. The results will be validated by time-domain simulations in 39 & 118 bus test systems, and the effectiveness of the proposed algorithm is validated by a cluster validity index, and also the results will be compared with other existing clustering methods. Finally, the conclusion is provided in section VIII.

II. GENERATOR COHERENCY BASED ON DYNAMIC COUPLING

For transient stability analysis, the network with n machines and connected representating graph is reduced to only the internal generator nodes (node behind the transient reactance), and all load and generator terminal buses are eliminated. If $\mathbf{Y_{bus}} = [Y_{ij}] = [G_{ij}+jB_{ij}]$ is the admittance matrix of the reduced network, then the behavior of this system in response to a disturbance can be expressed by [10]:

$$\begin{cases} 2H_i\ddot{\delta}_l = P_{mi} - P_{ei} \\ P_{ei} = E_i^2 G_{ii} + \sum_{j=1, j\neq i}^{n} E_i E_j (B_{ij}\sin\delta_{ij} + G_{ij}\cos\delta_{ij}) \end{cases} \quad (1)$$

where δ_i, H_i, E_i, P_{mi}, P_{ei} are rotor angle, inertia constant, internal generated voltage, input mechanical power and electrical power of generator i respectively and δ_{ij} is the relative angle between generators i and j. By linearizing above equations and neglecting the mutual conductance (G_{ij}), the small deviation of rotor angle of generator i can be obtained from:

$$2H_i\ddot{\delta}_{l\Delta} = -\sum_{j=1, j\neq i}^{n} K_{ij}\delta_{j\Delta} \quad (2)$$

$$K_{ij} = \left.\frac{\partial P_{ij}}{\partial \delta_{ij}}\right|_{\delta_{ij0}} = E_i E_j B_{ij}\cos\delta_{ij0} \quad (3)$$

Above equations can also be formulated by matrices: (Hereafter, all matrices are denoted by bold letters.)

$$2\mathbf{H}\ddot{\boldsymbol{\delta}}_{\boldsymbol{\Delta}} = -\mathbf{K}\boldsymbol{\delta}_{\boldsymbol{\Delta}} \quad (4)$$

$\mathbf{H}$ is a diagonal matrix of the inertia coefficients of generators and $\mathbf{K} = [K_{ij}]$ with diagonal entries defined as:

$$K_{ii} = -\sum_{j=1, j\neq i}^{n} K_{ij} \quad (5)$$

$K_{ij}/2H_i$ in (2) is interpreted as the acceleration of the rotor angle of machine i due to a change in rotor angle of machine j. According to the definition [42], two generators are exactly coherent if the rotor acceleration of two generators due to a disturbance is the same. Although exact coherency is an ideal concept and rarely occurs in real power systems, it was shown in [7] that after a disturbance there is an inherent tendency to a strong dynamic coupling among some machines in the same CG while swinging against other groups with inter-area weak coupling. Therefore, this study proposes a coherency criterion for the concept of dynamic coupling [43]. The similarity function between generators i and j is defined as:

$$w_{ij} = \left(\frac{1}{H_i} + \frac{1}{H_j}\right) E_i E_j B_{ij}\cos\delta_{ij0} \quad (6)$$

where w_{ij} is the dynamic coupling between generators i and j. Then this study employs the slow coherency as the coherency measure in a measurement-based method. Above similarity function indicates that generators with smaller inertia constants and larger admittance of reduced network (hence, smaller impedance) results in a larger coherency value, which the latter reflects the effect of weak connections in power system on slow coherency.

III. BACKGROUND ON SUPPORT VECTOR CLUSTERING

SVC technique was inspired by the concept of Support Vector Machine (SVM) that is generally used for classification of data points [44]. The idea of using a hyperplane in feature space for classifying the data points was extended in [45] with formulating the new idea of using a hypersphere to find the domain description of a dataset [45]; however, it was observed in [41] that the same formulation framework could be applied to solve a clustering problem. The main idea of SVC is that if the data points in the original data space, as shown in Fig. 1 are mapped into a higher dimensional feature space by a nonlinear transformation (φ), the minimum sphere in the feature space, which encloses all the data points, is found and transformed back to the original space, the obtained contours in original data space represent the boundaries of the clusters [41].

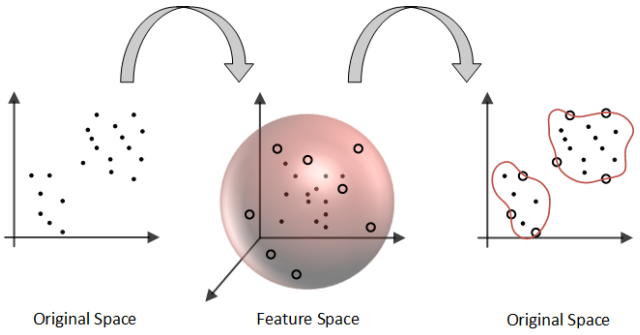

FIGURE 1. Transformation of data points to feature space.

Assume $\{x_i\} \subset X$, $i = 1, \ldots, N$ is a dataset with $X \subset R^d$, the d-dimensional data space. An unknown nonlinear transformation (φ) maps the data points to the feature space. The minimal sphere that contains all the points in this space, is described by:

$$\|\phi(x_i) - a\|^2 \leq R^2 + \xi_i \quad \forall i, \tag{7}$$

where a and R are the center and radius of the enclosing sphere and ξ_i is a slack variable for applying a soft margin constraint to the optimization problem that can be formulated as:

$$\begin{cases} \min R^2 + C \sum_i \xi_i \\ s.t.\ \|\phi(x_i) - a\|^2 \leq R^2 + \xi_i \quad \forall i, \xi_i > 0 \end{cases} \tag{8}$$

where C is the penalty constant that incorporates the total violation of the constraints. For solving this problem, the Lagrangian function is employed, and it is shown in [41] that by applying Karuch-Kuhn-Tucker conditions, a data point known as Boundary Support Vectors (BSV) with $\xi_i > 0, \beta_i = C$ is located outside the sphere in the feature space. If $\xi_i = 0, \beta_i > 0$, the point lies on the surface of the sphere and is called Support Vector (SV) and if $\xi_i = 0$, $\beta_i = 0$, the point is located inside the minimal sphere. It is also found that if $C \geq 1$, no BSV will exist, i.e., outlier are not allowed to appear in the data set. By applying the above conditions to the primal optimization problem, it can be transformed to a dual problem with the same solution.

$$\begin{cases} \max \sum_i \beta_i \phi(x_i)^2 - \sum_{i,j} \beta_i \beta_j \phi(x_i)\phi(x_j) \\ s.t.\ 0 \leq \beta_i \leq C, \quad \sum_i \beta_i = 1 \end{cases} \tag{9}$$

By finding an appropriate Kernel function that satisfies Mercer theorem [46], dot products can be expressed by the Kernel function. Gaussian Kernel function was employed in this study, i.e., $K(x_i, x_j) = \exp\left(-q \|x_i - x_j\|^2\right)$ with q as width parameter and $\|.\|$ indicating the Euclidean distance; therefore, the optimization problem can be expressed as below.

$$\begin{cases} \max \sum_i \beta_i K(x_i, x_i) - \sum_{i,j} \beta_i \beta_j K(x_i, x_j) \\ s.t.\ 0 \leq \beta_i \leq C, \quad \sum_i \beta_i = 1 \end{cases} \tag{10}$$

The dual problem has only β_is as unknowns and can be solved by a quadratic programming solver with choosing appropriate values for q and C [47]. Then for any point x in the data space, the distance of the image of this point in the feature space from the center of the sphere is obtained from:

$$R^2(x) = \|\phi(x) - a\|^2 = K(x, x) - 2\sum_i \beta_i K(x_i, x) + \sum_{i,j} \beta_i \beta_j K(x_i, x_j) \tag{11}$$

Then, the radius of the sphere is:

$$R = \{R(x_i) \,|x_i \text{ is SV}\} \tag{12}$$

The enclosing contours of the points in the original data space are expressed by a set of points:

$$\{x \,|R(x) = R\} \tag{13}$$

Then in cluster labeling stage, all points are assigned to distinct clusters [41]. Based on a proximity graph-based method [41], given any pair of points in data space, the connecting path is divided into several points (e.g. 10 points in this study), and if all the corresponding images in the feature space located inside the minimal sphere, the points in data space belong to the same cluster. An adjacency matrix, $\mathbf{A} = [a_{ij}]$, is formed which a_{ij} indicates that a pair of data points i and j belong to the same cluster or not:

$$a_{ij} = \begin{cases} 1 & \text{if } \forall \lambda \in [0, 1], R\left(\lambda x_i + (1 - \lambda) x_j\right) \leq R \\ 0 & \text{otherwise} \end{cases} \tag{14}$$

Finally, the clusters are formed as the connected components of the graph defined by $\mathbf{A}$. A critical issue in SVC algorithm is choosing appropriate values for width parameter of Gaussian function (q) and soft margin constant (C). It was demonstrated in [41] that how variations of q and C have effects on the boundaries of clusters and the number of outliers respectively. In this study, an algorithm for the automatic setting of the values of q and C is used to achieve the optimal clustering result [48].

IV. EMBEDDING THE DATA IN EUCLIDEAN SPACE: PRE-PROCESSING THE DATA

In order to identify the coherent generators from dynamic coupling, it is necessary to adopt a distance measure for the SVC from the defined pairwise similarity between generators. Generally, *metric* distance measures are fundamental to machine learning-based algorithms such as SVC to manipulate the datasets; therefore, non-metric distance measure defined on the pairwise similarity of data points must be necessarily translated to an appropriate metric distance to be usable. The Gaussian function employed in the SVC algorithm needs the Euclidean distance between the points; however, the dissimilarity or distance matrix, obtained from the dynamic coupling analysis of generators is not intrinsically a *metric* distance measure. Embedding will translate the defined non-metric pairwise similarity of data points into a Euclidean space [49]. Therefore, embedding will find the points in the Euclidean space such that their distance in this space is equal to the calculated dissimilarity values of generators obtained from the dynamic coupling study. Then as shown in Fig. 2, the resultant points act as the input dataset given to the clustering algorithm to be clustered according to their Euclidean distances. In this study, a method that can be interpreted as Kernel Principal Component Analysis (KPCA) is used for embedding. KPCA is a nonlinear extension of PCA [50], and is applied to find the principal components of the data in Euclidean space. Then the principal components are used to identify a dataset in Euclidean space, which preserves the defined distance between the input data points. The data embedded in the low dimensional Euclidean space are non-linearly related to the high dimensional input data. The difference of KPCA with the conventional PCA method is that in the former method, the input data are mapped to a feature space by a nonlinear kernel function and then PCA is employed to extract the principal components of data in the feature space. The detail of the embedding procedure is as follows.

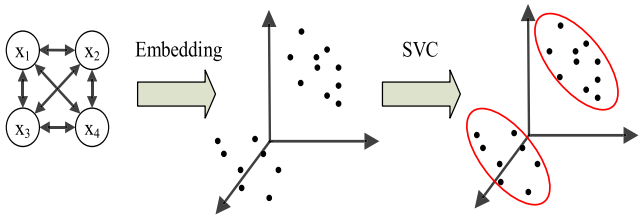

FIGURE 2. Steps of embedding and clustering the input dataset.

According to the definition [49], the distance matrix $\mathbf{D} = [d_{ij}]$ is Euclidean if and only if n points can be found in the Euclidean space such that the Euclidean distance between points i and j is d_{ij}. Embedding into a Euclidean space is possible only if the distance matrix is Euclidean. Moreover, it was proved [51] that if the similarity matrix $\mathbf{S} = [s_{ij}]$ is positive semi-definite (p.s.d) with $0 \leq s_{ij} \leq 1$ and $s_{ii}=1$, then the distance matrix $\mathbf{D} = [d_{ij}]$ with $d_{ij} = \sqrt{1 - s_{ij}}$ is Euclidean. Therefore, if we can define a similarity measure such that the distance matrix is p.s.d, embedding the points into a Euclidean space is possible. In this study, the similarity matrix is constructed in the format of a normalized Laplacian matrix since it was shown in [52] that the Laplacian matrix is p.s.d:

$$\mathbf{S} = \mathbf{G}^{-\frac{1}{2}} (\mathbf{G} - \mathbf{W}) \mathbf{G}^{-\frac{1}{2}} \tag{15}$$

where $\mathbf{W}$ is Coupling matrix with entries (w_{ij}) equal to the dynamic coupling of generators i, j and $\mathbf{G}$ is Degree matrix which is a diagonal matrix with $g_{ii} = \sum_{j=1}^{n} w_{ij}$.

Having defined the similarity matrix such that the dataset is embeddable in Euclidean space, the dataset is embedded in Euclidean space according to the procedure shown in Fig. 3. As shown, the next step is to compute matrix $\mathbf{C}$ from the squared distance matrix. $\mathbf{C}$ is the covariance matrix of the data points in the Euclidean space and can act as the kernel function in the proposed KPCA-based method.

$$\mathbf{C} = -\frac{\mathbf{1}}{\mathbf{2}} \mathbf{Q} \mathbf{D_{sq}} \mathbf{Q}, \quad \mathbf{D_{sq}} = [d_{ij}^2] \tag{16}$$

where $\mathbf{Q}$ is centering matrix defined as:

$$\mathbf{Q} = \mathbf{I} - \frac{1}{n} \mathbf{e} \mathbf{e^t} \tag{17}$$

n is the number of points; $\mathbf{I}$ is unity matrix, and $\mathbf{e}$ is a column vector of ones. Similar to KPCA method, the eigen-decomposition of matrix $\mathbf{C}$ gives the desired data points in the Euclidean space. The eigenvalues and eigenvectors of $\mathbf{C}$ are obtained in the next step.

$$\mathbf{C} = \mathbf{V} \mathbf{\Lambda} \mathbf{V^t} \tag{18}$$

in which, $\mathbf{V} = [\mathbf{v_1}\ \mathbf{v_2} \ldots\ \mathbf{v_n}]$ is row matrix of eigenvectors v_i, and Λ is a diagonal matrix of eigenvalues. The points in the Euclidean space are obtained from:

$$\mathbf{X} = \mathbf{V} \mathbf{\Lambda}^{1/2} \tag{19}$$

which $\mathbf{X}$ contains the corresponding n data points in n-dimensional Euclidean space as the row vectors of the matrix. Finally, the resultant dataset is given to the SVC algorithm as the input data, and SVC will identify the distinct clusters of this new dataset.

V. PROPOSED ALGORITHM FOR COHERENCY IDENTIFICATION

Fig. 4 presents the overall view of the proposed procedure to separate the coherent generators in a real-time application. It is assumed that the whole network is fully observed through PMUs installed at all buses, and the Synchrophasor data are obtained for the last time window T which is long enough to monitor the slow oscillations of generators. Furthermore, the groupings of generators are updated every time step $\Delta T < T$. The algorithm shown in Fig. 4 demonstrates the steps required for the time step ΔT. The first step is to compute the similarity values between any generator pair according to (6) for the last time window T. Therefore, the input data of the clustering algorithm is an $n_g \times n_g$ distance matrix (n_g is the

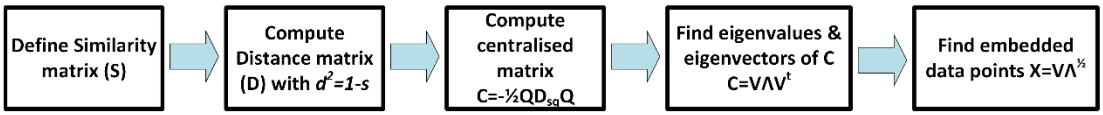

FIGURE 3. Steps of embedding the input data into the Euclidean space.

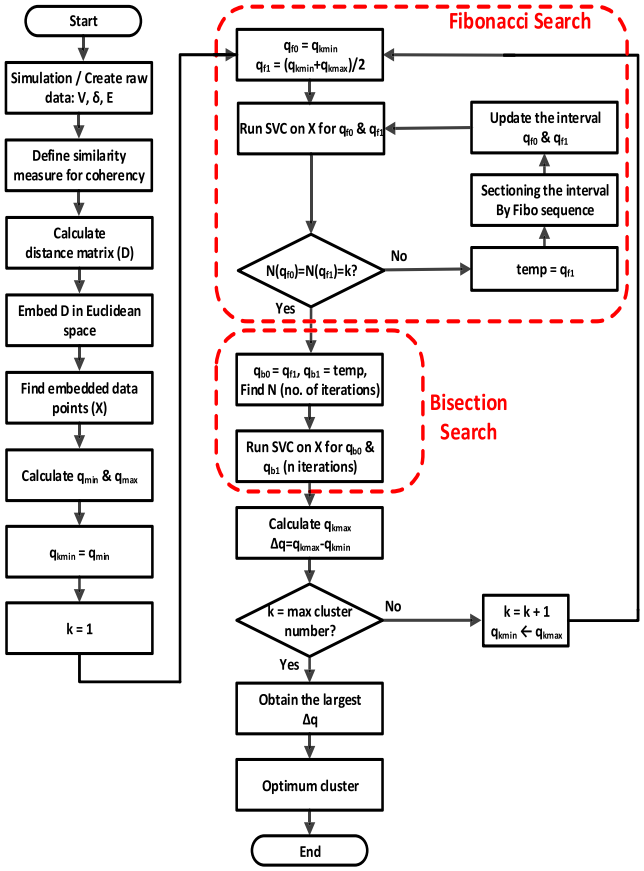

FIGURE 4. Proposed clustering flowchart.

number of generators). The SVC technique with parameter selection and cluster validity method that previously verified in [48] was implemented to achieve the optimal cluster structure. The proposed algorithm in this study for the coherency detection is robust against noise or outliers. If the input dataset contains some noise signals, this noise is eliminated during preprocessing stage, when the input dataset is embedded in the Euclidean space. The reason is that the KPC-based technique orders the principal components of high-dimensional dataset by their eigenvalues, then picks a number (in here, n_g) of largest eigenvalues that cover larger possible variance, and neglects the noise with the lowest eigenvalues, hence smaller variance. Moreover, the SVC method is the best option to deal with the outliers due to its robustness to outliers. Generally, soft constraint parameter, C, in SVC algorithm allows exclusion of outliers or inclusion of singleton clusters in the cluster structure. In this study, soft constraint parameter is considered $C=1$ because it is required to assign every generator to a cluster, and no generator is allowed to be unattended. In this method, SVC is carried out repeatedly for several iterations, and the width parameter (q) is automatically set at each iteration to result in the best possible clustering result. The key point used as the cluster validity measure was that every cluster number corresponds to a q interval, and the optimal cluster corresponds to the largest q interval [48]. The reason for this phenomenon comes from the fact that the boundaries of the clusters change by variation of q. It was observed that by increasing q, the tightness of the contours of cluster boundaries, and also the number of SVs increases gradually, until the current contours split into smaller contours, consequently the number of clusters increases [48].

By adopting this approach, there is no need to evaluate a conventional cluster validity index at each q step anymore, and hence, the total number of iterations is considerably reduced. According to Fig. 4, the first step, after the dataset is embedded, is to find the search range of $q_r = [q_{min}, q_{max}]$ [41]:

$$q_{min} = \frac{1}{\max\limits_{1\le i,j\le n} \|x_i - x_j\|^2}, \quad q_{max} = \frac{1}{\min\limits_{1\le i,j\le n} \|x_i - x_j\|^2} \tag{20}$$

There is also a maximum number of clusters defined based on practical considerations of the network operator. The simplest heuristic search method to find the largest q interval is to divide q_r into several intervals regarding an assumed accuracy and run the SVC at the mean value of each interval, but the number of iterations would be too large with this method in large search ranges, which is not feasible in real-time applications. To avoid excessive iterations, it is proposed to implement the previously introduced search method combining both Fibonacci and Bisection search techniques with the minimum number of iterations [48]. The parameters and details of Fibonacci and bisection search were chosen and performed according to [47]. Assuming the number of clusters obtained from an SVC run with q is n_i ($N(q) = n_i$), Fibonacci search technique is used to find any two points in the overall search range with the same number of clusters, i.e., $N(q_{f0}) = N(q_{f1}) = n_i$, and Bisection search technique is used to locate the approximate point that n_i changes. The SVC is carried out for every Fibonacci iteration within the range $[q_{f0}, q_{f1}]$ and also for every Bisection iteration within the range $[q_{b0}, q_{b1}]$. The procedure starts with $q_{f0} = q_{min}$ and $q_{f1} = 0.5(q_{min} + q_{max})$. During the Fibonacci search, once two points with the same number of clusters are located, the Fibonacci search stops temporarily and the procedure enters a bisection search to find the lower and upper bounds of the associated interval for each cluster number. After the interval bounds are found, q_{min} is updated, and the same procedure is repeated for

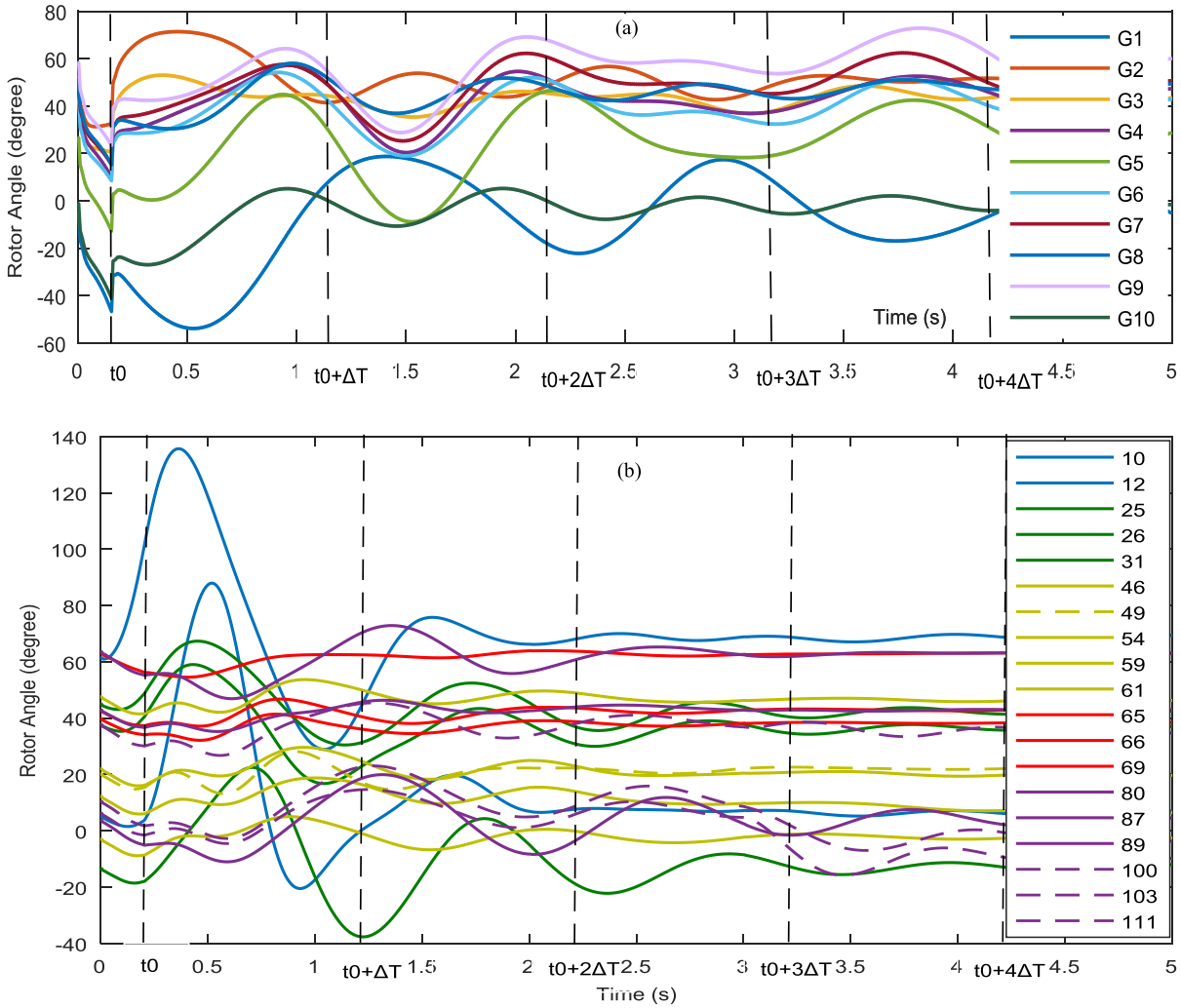

FIGURE 5. Rotor angle of generators during the defined scenarios in a) 39 bus b) 118 bus.

finding the next q interval until all intervals are covered and the optimal clustering structure is provided as the clustering result associated with the largest interval.

VI. RESULTS AND DISCUSSIONS

The efficacy of the proposed algorithm is demonstrated through time domain simulation of defined events in 39 bus and 118 bus test systems. The scenarios are based on the assumption that all the rotor angle and voltage magnitude of generators are obtained from the PMUs installed at all generator buses.

Bus 31 and Bus 69 were considered as slack buses in 39 bus and 118 bus system respectively. Full observability was assumed for both test systems with the sampling rate of 50 Hz. Moreover, to detect the low frequency oscillations, the coherency analysis is carried out over the last time window of $T = 10$ s and it is updated for every time step $\Delta T = 1$ s following the fault; therefore the CGs are updated. The dominant interarea modes are generally within the range of 0.1-0.8 Hz, thus a time window $T = 10$ s is suitable to capture even the slowest modes [53].

A. TEST SYSTEM I: NEW ENGLAND 39 BUS

The data of components of 39 bus power system were taken from [54]; however, the parameters of synchronous generators including the power ratings and inertia constants were adapted to achieve realistic inertia time constants and to allow the power dispatch within reasonable governor limits. A three-phase short circuit was created at the middle point of line 4-14 at $t = 0$ s, then the fault is cleared by opening the faulty line after 0.15 s and the line 16-17 is tripped at $t = 2.1$ s due to overloading. The oscillations of all ten generators are demonstrated in Fig. 5a. The instant of fault clearing (t_0) was assumed to be the reference time for coherency study.

Based on the calculated dynamic coupling between generators, the pairwise distance values of generators are computed according to (15). Fig. 6 displays the pairwise distance values as color image plots to better demonstrate the coupling of generators over the time window T at three consecutive time steps after the disturbance. The smaller the distance (the larger the similarity) between the generators, the darker is the corresponding square in the color plot. It can be seen from Fig. 6(a) that the G2, G3 show strong coupling,

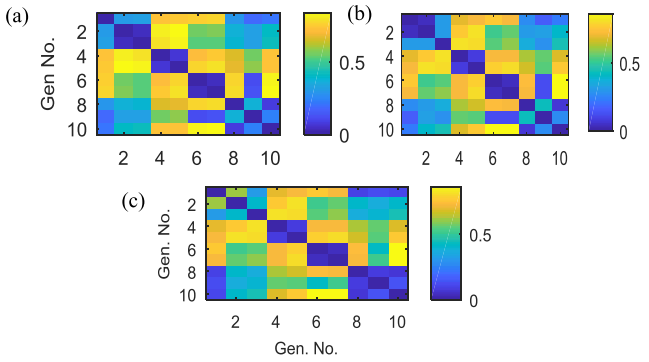

FIGURE 6. Color plots of distance matrix for 39 bus system. a) At $t_0 + \Delta T$. b) At t_0+2ΔT. c) At t_0+3ΔT.

while G4, G5 are coupled together as well as G6, G7. It is obvious that all diagonal units must be blue indicating the maximum possible coupling because the distance of a generator with respect to itself is zero. It is evident from Fig. 6(b) that 1 s after the fault, the coupling between G2 and G3 weakens while G1 shows a tendency to make a strong connection with G2.

After the distance matrix is constructed for the current time window, it is then used to embed the data points in the Euclidean space. The three principal components of the rotor angles in the new space are depicted in Fig 7. The clustering algorithm is applied to the embedded data points to cluster the data points with the optimal number of CGs of generators, which is found to be five for the first time step. Generally, the generators with closer distances may have stronger coupling due to the effect of impedance in synchronizing coefficient, however during a short time dynamic response of the generators, this grouping can change, and a generator may jump off a CG and join another group regarding the dynamic change in acceleration of rotor angles. The dynamic behavior of generators following the events are better demonstrated in Fig. 8. It was observed that the clustering procedure initially grouped the generators in five groups of {G1}, {G2, G3}, {G4, G5}, {G6, G7, G9}, and {G8, G10}.

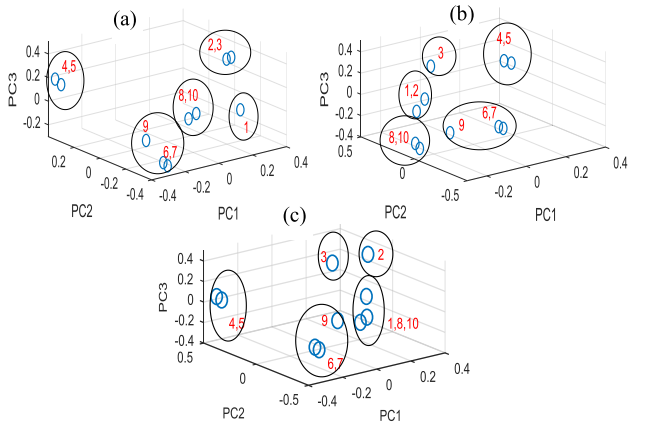

FIGURE 7. Principle components of rotor angles embedded in Euclidean space for 39 bus system. a) At $t_0 + \Delta T$. b) At t_0+2ΔT. c) At t_0+3ΔT.

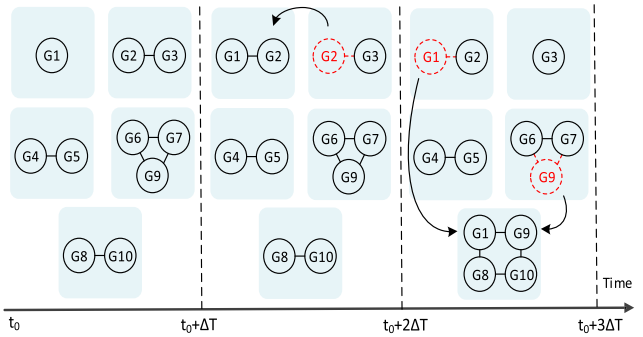

FIGURE 8. The change of CGs in 39 bus system over time.

After the second time step, the grouping is updated such that G2 separates from G3 and joins G1 to form a new CG while G3 becomes a cluster containing a single generator. Then after t=2.1 s, disconnecting the line 16-17 weakens the strong tie between {G9} and {G6, G7}. Hence, G9 leaves its CG and tends to oscillate with {G8, G10}. Similarly, G1 joins this group and {G1, G8, G9, G10} form a group of generators swinging together.

Once the original data space is embedded in the Euclidean space, SVC algorithm is initiated by setting the values of both q and C parameters. Since it is expected to assign every single generator to a CG, without invoking any outliers, C is taken to be 1 while q is iteratively changed until the optimal q associated with the optimal cluster number is achieved. For the first time step, the minimum and maximum values of q are computed from (20) as $q_{min} = 1.13$ and $q_{max} = 6912.7$ to identify the initial search range for q.Δ= 0.1 was chosen for the final uncertainty interval of both Fibonacci and Bisection search methods and ε= 0.01 for the reduction factor in the uncertainty interval of Fibonacci method. Fig. 9(a) shows the relation between the number of clusters and q obtained by SVC. As seen, the optimal number of clusters is five for the first time step, which is corresponding to the q interval [1030.8, 1888.2] with Δq=857.4. In comparison with the case that all values of q within [1.13, 6912.7] are investigated at every $q = 0.1$ (because it was assumed that $\Delta = 0.1$), it can be shown that the total number of SVC iteration decreased considerably and it speeds up the computation procedure.

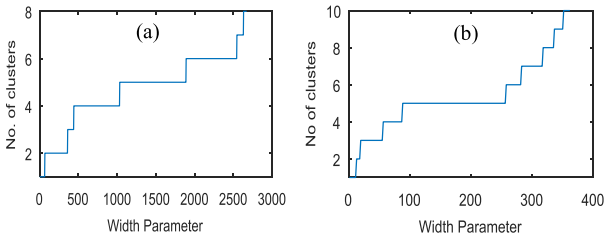

FIGURE 9. No. of clusters vs. q parameter in SVC. a) 39 bus. b) 118 bus.

B. TEST SYSTEM II: IEEE 118 BUS

A three-phase short circuit was defined on the line 8-30 close to bus 8. Without considering autoreclosing, the fault was cleared after 0.2 s by opening the corresponding line.

Then the lines 49-51, 100-103 and 103-104 were tripped at t=2 s, t=3 s, t=3.2 s, respectively, due to overloading protection. The post-disturbance behavior of rotor angle of generators is depicted in Fig. 5(b). The curves with dash lines are for the generators that change their CGs over the investigated time, according to the proposed algorithm. The grouping result after four consecutive time steps is also presented in Table 1. The proposed SVC technique has the advantage of automatic identification of the best partition number. Finding the optimal number of partitions of the generators is found to be five, as shown in Fig. 9(b), which corresponds to the q interval [86.79, 255.96] with Δq=*169.2*. The results indicate that once the coherency of generators is identified after the first event, it doesn't change until the second event happens at t=2 s. After the first event, five coherent areas are initially identified while after the second event generator 49 changes its cluster to group 4, and after the third event, group 5 splits into two different clusters. The offline studies show that generators 10, 12, 25, 26, 31 have a natural tendency to swing together [40], however, in this case, disconnecting the line 8-30 weakens the inherent dynamic coupling of these generators and causes two distinct groups of 10, 12 and 25, 26, 31 swing against each other and also the other CGs as shown in Fig. 5(b). Then immediately after the occurrence of the second event at t=2 s, opening the line 49-51 cuts the loose coupling between the generator 49 and the rest of generators in its CG. Following a disturbance in the network, a significant change in the dynamic operating condition of the grid induces a change in the coupling between the generators, hence, in this particular scenario, the generator 49 separates from its group and joins the groups of generator 65, 66, 69. Similarly, immediately after opening the line 100-103 and 103-104, the group consisting the generators 80, 87, 89, 100, 103, 111 splits into two groups, while 80, 87, 89 swing in one group against 100, 103, 111.

TABLE 1. Clustering result for 118 bus system.

Time	Group 1	Group 2	Group 3	Group 4	Group 5	Group 6
t_0+ΔT	10,12	25,26,31	46,49,54,59,61	65,66, 69	80,87,89,100, 103,111	-
t_0+2ΔT	10,12	25,26,31	46,49,54,59,61	65,66,69	80,87,89,100, 103,111	-
t_0+3ΔT	10,12	25,26,31	46,54,59,61	49,65,66,69	80,87,89,100, 103,111	-
t_0+4ΔT	10,12	25,26,31	46,54,59,61	49,65,66,69	80,87,89	100,103, 111

Fig. 10 show the color plots of distance values for the 1st and 4th time steps to demonstrate the change of coherent groups (For simplicity, generators are numbered from 1 to 19 instead of showing the bus numbers). Several bluish patches of square units are identifiable in the plot, which means that these generators form different coherent clusters. The dataset representing the generators with calculated pairwise similarity values (after the 1st time step) are embedded in Euclidean space, and the three first principal components of this new dataset are depicted in Fig. 11.

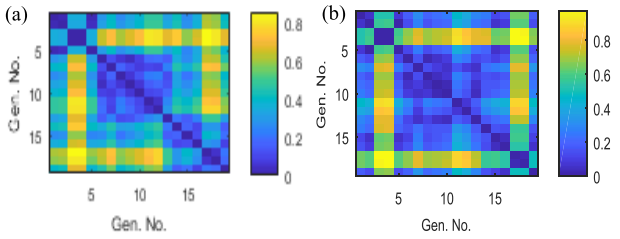

FIGURE 10. Colour plots of distance matrix for 118 bus system. a) At $t_0 + \Delta T$. b) At t_0+4ΔT.

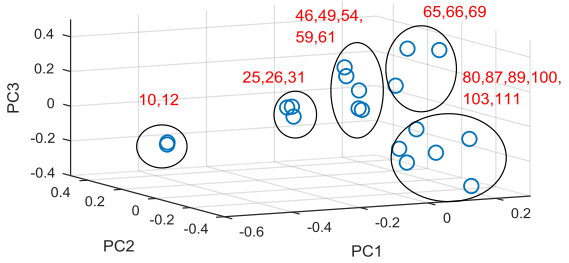

FIGURE 11. Principle components of rotor angles embedded in the Euclidean space, 118 bus grid, the first time step.

VII. VALIDATION OF GENERATOR GROUPING AND COMPARATIVE ANALYSIS

The average silhouette width is employed to validate the grouping of the generators obtained by the proposed clustering algorithm. The silhouette width of any data point i (S_i) represents how similar is this point to other points that are already grouped in the same cluster and how distant are the points in a cluster to other neighboring clusters. S_i is defined as [55]:

$$S_i = \begin{cases} 1 - a_i/b_i & \text{if } a_i < b_i \\ 0 & \text{if } a_i = b_i \\ b_i/a_i - 1 & \text{if } a_i > b_i \end{cases} \quad (21)$$

where a_i is the average distance of i to all other points within its cluster, and b_i is the smallest average distance of i to all points in any other cluster of which i is not a member. The overall silhouette width of a cluster structure (or shortly silhouette value) reflects both the compactness of dataset within the clusters and separation from neighboring clusters in a single value. From the above definition, $-1 \leq S_i \leq 1$. It is noted that if the dataset is well clustered, S_i tends to be larger than the cases with poorer cluster quality. Fig. 12 shows five silhouette plots of CGs for different cluster numbers during the first time interval of 39 bus oscillation scenario. It can be seen from Fig. 12(a) that the overall silhouette value for the case with two CGs is 0.485, which means the generators are not well clustered. As seen in Fig. 12(b)-(e), by incrementing the number of groups, the overall silhouette values are obtained as 0.725, 0.741, 0.817 and 0.793 for 3, 4, 5 and 6 coherent groups, respectively. Therefore the proper number of coherent groups should be five for the 1st time interval with maximum silhouette value which means the generators are better separated concerning their dynamic coupling in comparison with other cluster structures. The results are in

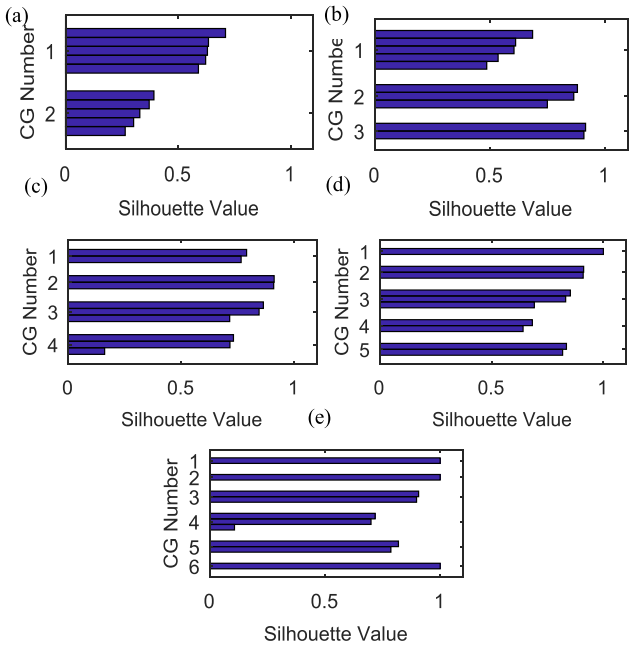

FIGURE 12. Silhouette plots of CGs for different numbers of groups in 39 bus system a) two b) three c) four d) five e) six clusters.

accordance with the output of the SVC algorithm, which was shown in Fig. 7(a).

To better demonstrate the efficiency of the proposed method (SVC method), it is compared with another measurement-based coherency identification method which was investigated in several studies [1], [29]. In this approach, the degree of coherency between any pair of generators is defined based on rotor speed deviation of generators. Spectral Clustering (SC), and Fuzzy C-means Clustering (FCM) were used to cluster the generators with the adopted coherency measure in [1] and [29], respectively. SC method is based on Eigenanalysis of the similarity matrix, and FCM is based on minimization of the within-cluster variances. FCM assigns each generator to multiple CGs with varying degrees of membership. Table 2 presents the clustering structure and overall silhouette values (S) of the first two intervals of 39 bus grid, resulted from different methods including the proposed method (SVC) in the present study.

TABLE 2. Clustering result for 39 bus system.

	Time	Group 1	Group 2	Group 3	Group 4	Group 5	S
SVC	t_0+ΔT	1	2,3	4,5	6,7,9	8,10	0.817
	t_0+2ΔT	1,2	3	4,5	6,7,9	8,10	0.809
FCM	t_0+ΔT	1	2,3	4,5,6,7,9	8	10	0.551
	t_0+2ΔT	1	3	4,5,6,7	9	2,8,10	0.632
SC	t_0+ΔT	1	2,3	4,5	6,7,9	8,10	0.817
	t_0+2ΔT	1	3	4,5	6,7,9	2,8,10	0.785

It is noticed that in both clustering methods the grid is split into five clusters of {1},{3},{4,5},{6,7,9}, {2,8,10} after the second updating time interval. It is seen that the generator 2 joined the group: {8,10} and the reason for this is that as shown in Fig. 13, the rotor speed of generator 2 came close to the group of {8,10} temporarily; however, generator 2 has stronger dynamic coupling with generator 3 over the

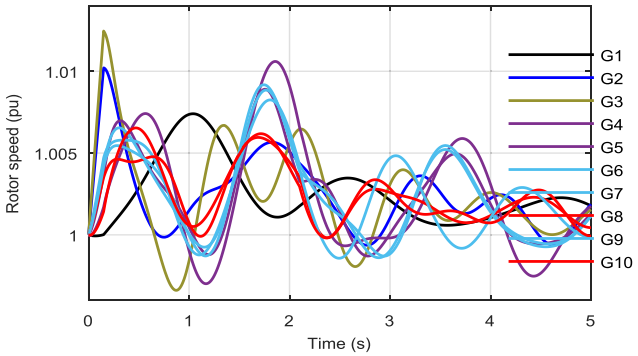

FIGURE 13. Rotor speed of generators with defined events in 39 bus system.

ten-second time window. The last column of table 2 compares all the overall silhouette values of cluster structures resulted from different methods. The higher values of S for SVC indicate the better quality of generator separation by the proposed SVC method. Therefore dynamic coupling as the coherency measure is a more reliable criterion than the speed deviation because it is possible to cluster the generators based on their slow coherency, rather than closeness of their rotor speeds. The reason why FCM method put two generators 8 and 9 in separate clusters while they showed strong dynamic coupling in both calculations and simulation results, or similarly joined the groups of {4,5},{6,7,9} can be explained by the dependence of FCM clustering algorithm on randomly selected initial centers of the clusters. Furthermore, both SC and FCM methods, the number of clusters must be specified before applying the algorithm whereas, in SVC algorithm, the optimal clustering solution and the proper number of CGs are achieved by a reliable search method. Comparison with other clustering methods reveals that the proposed method results in more reliable coherent groups, also with the advantage of identifying the proper number of clusters automatically.

Finally, the computational efficiency of proposed method is investigated, since the method is supposed to be implemented in online applications. The computation times of 39-bus and 118-bus test cases for a particular disturbance in each test case are listed in Table 3. The running times are also compared among different methods as recorded in MATLAB 2017a using Intel Core i7-6700 with 16 GB RAM. The results show that despite other methods (FCM, SC) cost less computation time, the proposed method is still suitable to be used in real-time applications, because running times, even in a laptop PC, is much lower than the updating time step $\Delta T = 1$ s. The running time of SVC is longer than FCM and SC due to applying the embedding, and SVC stages that both are time costly procedures. Despite this fact, considering other advantages of SVC method such as more reliable

TABLE 3. Computational time of test cases.

	FCM	SC	SVC
39-bus	0.003 s	0.010 s	0.051 s
118-bus	0.005 s	0.029 s	0.283 s

clustering result, robustness to noise/outlier, and providing automatically identified number of clusters, the proposed method is more suitable option for coherency detection.

VIII. CONCLUSION

In this study, a generator coherency identification methodology was proposed for online application based on measurement of voltages and angles obtained from PMUs, which is of vital importance in implementing the protective schemes of power system such as controlled islanding or wide area control. In this study, the dynamic coupling of generators, which was defined based on the acceleration of generators after a disturbance, was considered as the coherency criterion. The algorithm included two main stages: embedding the original dataset in Euclidean space and then performing the SVC clustering technique on the embedded dataset to identify the coherent generators. It was shown that by clustering the generators based on their slow coherency, it is possible to discover the consistent oscillatory pattern of generators. The most important feature of the proposed framework for coherency analysis is its efficacy to identify the optimal number of clusters. It was found that in contrast to other clustering methods, the proposed method is independent of a priori knowledge about the number of clusters and is able to choose the best option systematically among all feasible clustering structures. The proposed method is also robust to noise or outliers. The noise is eliminated during the embedding stage and the existence of outliers can be controlled by the soft constraint parameter of SVC. Finally, the clustering results were verified by a cluster validity measure that was defined based on the compactness of each cluster and separation between clusters, and it was observed that the proposed algorithm has an advantage over other coherency detection methods in the reliable grouping of generators with stronger dynamic coupling. The computational efficiency of the proposed algorithm was also investigated and it was shown that it is suitable to be implemented in real-time applications. Another interesting aspect of the study is that an embedding strategy incorporated in a clustering algorithm can also be applied to other clustering applications such as power network partitioning and controlled islanding after an appropriately chosen dissimilarity measure is adopted which is not even a metric distance measure.

REFERENCES

[1] A. Thakallapelli, S. J. Hossain, and S. Kamalasadan, "Coherency and online signal selection based wide area control of wind integrated power grid," *IEEE Trans. Ind. Appl.*, vol. 54, no. 4, pp. 3712–3722, Jul./Aug. 2018.

[2] A. Vahidnia, G. Ledwich, E. Palmer, and A. Ghosh, "Generator coherency and area detection in large power systems," *IET Gener., Transmiss. Distrib.*, vol. 6, no. 9, pp. 874–883, Sep. 2012.

[3] J. G. Slootweg and W. L. Kling, "The impact of large scale wind power generation on power system oscillations," *Electr. Power Syst. Res.*, vol. 67, no. 1, pp. 9–20, 2003.

[4] D. Gautam, V. Vittal, and T. Harbour, "Impact of increased penetration of DFIG-based wind turbine generators on transient and small signal stability of power systems," *IEEE Trans. Power Syst.*, vol. 24, no. 3, pp. 1426–1434, Aug. 2009.

[5] T. Sadamoto, A. Chakrabortty, T. Ishizaki, and J.-I. Imura, "Retrofit control of wind-integrated power systems," *IEEE Trans. Power Syst.*, vol. 33, no. 3, pp. 2804–2815, May 2018.

[6] F. Hashiesh, H. E. Mostafa, A.-R. Khatib, I. Helal, and M. M. Mansour, "An intelligent wide area synchrophasor based system for predicting and mitigating transient instabilities," *IEEE Trans. Smart Grid*, vol. 3, no. 2, pp. 645–652, Jun. 2012.

[7] B. Avramovic, J. Chow, P. Kokotovic, G. Peponides, and J. Winkelman, *Time-Scale Modeling of Dynamic Networks With Applications to Power Systems* (Lecture Notes in Control and Information Sciences), vol. 46. New York, NY, USA: Springer-Verlag, 1982.

[8] H. You, V. Vittal, and X. Wang, "Slow coherency-based islanding," *IEEE Trans. Power Syst.*, vol. 19, no. 1, pp. 483–491, Feb. 2004.

[9] B. P. Padhy, S. C. Srivastava, and N. K. Verma, "A coherency-based approach for signal selection for wide area stabilizing control in power systems," *IEEE Syst. J.*, vol. 7, no. 4, pp. 807–816, Dec. 2013.

[10] J. H. Chow, *Power System Coherency and Model Reduction*. New York, NY, USA: Springer, 2013.

[11] O. Gomez and M. A. Rios, "Real time identification of coherent groups for controlled islanding based on graph theory," *IET Gener., Transmiss. Distrib.*, vol. 9, no. 8, pp. 748–758, 2015.

[12] I. Kamwa, A. K. Pradhan, and G. Joos, "Automatic segmentation of large power systems into fuzzy coherent areas for dynamic vulnerability assessment," *IEEE Trans. Power Syst.*, vol. 22, no. 4, pp. 1974–1985, Nov. 2007.

[13] R. Podmore, "Identification of coherent generators for dynamic equivalents," *IEEE Trans. Power App. Syst.*, vol. PAS-97, no. 4, pp. 1344–1354, Jul. 1978.

[14] J. R. Winkelman, J. H. Chow, J. J. Allemong, and P. V. Kokotovic, "Multi-time-scale analysis of a power system," *Automatica*, vol. 16, no. 1, pp. 35–43, 1980.

[15] X. Wang, V. Vittal, and G. T. Heydt, "Tracing generator coherency indices using the continuation method: A novel approach," *IEEE Trans. Power Syst.*, vol. 20, no. 3, pp. 1510–1518, Aug. 2005.

[16] G. Xu and V. Vittal, "Slow coherency based cutset determination algorithm for large power systems," *IEEE Trans. Power Syst.*, vol. 25, no. 2, pp. 877–884, May 2010.

[17] A. Chakrabortty, J. H. Chow, and A. Salazar, "A measurement-based framework for dynamic equivalencing of large power systems using wide-area phasor measurements," *IEEE Trans. Smart Grid*, vol. 2, no. 1, pp. 68–81, Mar. 2011.

[18] G. Chavan, M. Weiss, A. Chakrabortty, S. Bhattacharya, A. Salazar, and F.-H. Ashrafi, "Identification and predictive analysis of a multi-area WECC power system model using synchrophasors," *IEEE Trans. Smart Grid*, vol. 8, no. 4, pp. 1977–1986, Jul. 2017.

[19] T. Hiyama, "Identification of coherent generators using frequency response," *IEE Proc. C-Gener., Transmiss. Distrib.*, vol. 128, no. 5, pp. 262–268, 1981.

[20] A. M. Khalil and R. Iravani, "Power system coherency identification under high depth of penetration of wind power," *IEEE Trans. Power Syst.*, vol. 33, no. 5, pp. 5401–5409, Sep. 2018.

[21] M. Jonsson, M. Begovic, and J. Daalder, "A new method suitable for real-time generator coherency determination," *IEEE Trans. Power Syst.*, vol. 19, no. 3, pp. 1473–1482, Aug. 2004.

[22] Z. Lin, F. Wen, Y. Ding, and Y. Xue, "Wide-area coherency identification of generators in interconnected power systems with renewables," *IET Gener., Transmiss. Distrib.*, vol. 11, no. 18, pp. 4444–4455, 2017.

[23] M. R. Salimian and M. R. Aghamohammadi, "Intelligent out of step predictor for inter area oscillations using speed-acceleration criterion as a time matching for controlled islanding," *IEEE Trans. Smart Grid.*, vol. 9, no. 4, pp. 2488–2497, Jul. 2018.

[24] S. Avdaković, E. Bećirović, A. Nuhanović, and M. Kušljugić, "Generator coherency using the wavelet phase difference approach," *IEEE Trans. Power Syst.*, vol. 29, no. 1, pp. 271–278, Jan. 2014.

[25] Y. Susuki and I. Mezic, "Nonlinear Koopman modes and coherency identification of coupled swing dynamics," *IEEE Trans. Power Syst.*, vol. 26, no. 4, pp. 1894–1904, Nov. 2011.

[26] N. Senroy, "Generator coherency using the Hilbert–Huang transform," *IEEE Trans. Power Syst.*, vol. 23, no. 4, pp. 1701–1708, Nov. 2008.

[27] J. Wei, D. Kundur, and K. L. Butler-Purry, "A novel bio-inspired technique for rapid real-time generator coherency identification," *IEEE Trans. Smart Grid*, vol. 6, no. 1, pp. 178–188, Jan. 2015.

[28] M.-H. Wang and H.-C. Chang, "Novel clustering method for coherency identification using an artificial neural network," *IEEE Trans. Power Syst.*, vol. 9, no. 4, pp. 2056–2062, Nov. 1994.
[29] S.-C. Wang and P.-H. Huang, "Fuzzy c-means clustering for power system coherency," in *Proc. IEEE Int. Conf. Syst., Man Cybern.*, vol. 3, Oct. 2005, pp. 2850–2855.
[30] I. Kamwa, A. K. Pradhan, G. Joos, and S. R. Samantaray, "Fuzzy partitioning of a real power system for dynamic vulnerability assessment," *IEEE Trans. Power Syst.*, vol. 24, no. 3, pp. 1356–1365, Aug. 2009.
[31] M. H. Rezaeian, S. Esmaeili, and R. Fadaeinedjad, "Generator coherency and network partitioning for dynamic equivalencing using subtractive clustering algorithm," *IEEE Syst. J.*, vol. 12, no. 4, pp. 3085–3095, Dec. 2018.
[32] K. K. Anaparthi, B. Chaudhuri, N. F. Thornhill, and B. C. Pal, "Coherency identification in power systems through principal component analysis," *IEEE Trans. Power Syst.*, vol. 20, no. 3, pp. 1658–1660, Aug. 2005.
[33] T. Jiang, H. Jia, H. Yuan, N. Zhou, and F. Li, "Projection pursuit: A general methodology of wide-area coherency detection in bulk power grid," *IEEE Trans. Power Syst.*, vol. 31, no. 4, pp. 2776–2786, Jul. 2016.
[34] Z. Lin, F. Wen, and Y. Ding, "Data-driven coherency identification for generators based on spectral clustering," *IEEE Trans. Ind. Informat.*, vol. 14, no. 3, pp. 1275–1285, Mar. 2018.
[35] C. Juarez, A. R. Messina, R. Castellanos, and G. Espinosa-Perez, "Characterization of multimachine system behavior using a hierarchical trajectory cluster analysis," *IEEE Trans. Power Syst.*, vol. 26, no. 3, pp. 972–981, Aug. 2011.
[36] M. Davodi, M. Banejad, A. Ahmadyfard, and M. O. Buygi, "Coherency identification using hierarchical clustering method in power systems," in *Proc. Int. Conf. Elect. Eng.*, 2008, pp. 1–6.
[37] Z. Lin, F. Wen, Y. Ding, Y. Xue, S. Liu, Y. Zhao, and S. Yi, "WAMS-based coherency detection for situational awareness in power systems with renewables," *IEEE Trans. Power Syst.*, vol. 33, no. 5, pp. 5410–5426, Sep. 2018.
[38] R. Agrawal and D. Thukaram, "Support vector clustering-based direct coherency identification of generators in a multi-machine power system," *IET Gener., Transmiss. Distrib.*, vol. 7, no. 12, pp. 1357–1366, 2013.
[39] M. Babaei, S. M. Muyeen, and S. Islam, "The impact of number of partitions on transient stability of intentional controlled islanding," in *Proc. 19th IEEE EEEIC Int. Conf. Environ. Elect. Eng.*, Genoa, Italy, 2019, pp. 1–6.
[40] L. Ding, F. M. Gonzalez-Longatt, P. Wall, and V. Terzija, "Two-step spectral clustering controlled islanding algorithm," *IEEE Trans. Power Syst.*, vol. 28, no. 1, pp. 75–84, Feb. 2013.
[41] A. Ben-Hur, D. Horn, H. T. Siegelmann, and V. Vapnik, "Support vector clustering," *J. Mach. Learn. Res.*, vol. 2, pp. 125–137, Mar. 2002.
[42] J. Machowski, J. Bialek, J. R. Bumby, and J. Bumby, *Power System Dynamics and Stability*. Hoboken, NJ, USA: Wiley, 1997.
[43] S. S. Lamba and R. Nath, "Coherency identification by the method of weak coupling," *Int. J. Elect. Power Energy Syst.*, vol. 7, no. 4, pp. 233–242, 1985.
[44] V. Vapnik, *The Nature of Statistical Learning Theory*. New York, NY, USA: Springer, 2013.
[45] D. M. J. Tax and R. P. W. Duin, "Support vector domain description," *Pattern Recognit. Lett.*, vol. 20, nos. 11–13, pp. 1191–1199, 1999.
[46] N. Cristianini and J. Shawe-Taylor, *An Introduction to Support Vector Machines and Other Kernel-Based Learning Methods*. Cambridge, U.K.: Cambridge Univ. Press, 2000.
[47] E. K. P. Chong and S. H. Zak, *An Introduction to Optimization*. Hoboken, NJ, USA: Wiley, 2013.
[48] J.-S. Wang and J.-C. Chiang, "A cluster validity measure with a hybrid parameter search method for the support vector clustering algorithm," *Pattern Recognit.*, vol. 41, no. 2, pp. 506–520, 2008.
[49] V. Von, "Non-metric pairwise proximity data," Ph.D. dissertation, Dept. Doctor Sci., Elect. Eng. Inform., Tech. Univ. Berlin, Berlin, Germany, 2004.
[50] B. Schölkopf, A. Smola, and K.-R. Müller, "Nonlinear component analysis as a kernel eigenvalue problem," *Neural Comput.*, vol. 10, no. 5, pp. 1299–1319, Jul. 1998.
[51] J. C. Gower and P. Legendre, "Metric and Euclidean properties of dissimilarity coefficients," *J. Classification*, vol. 3, no. 1, pp. 5–48, 1986.
[52] U. von Luxburg, "A tutorial on spectral clustering," *Statist. Comput.*, vol. 17, no. 4, pp. 395–416, 2007.
[53] M. Klein, G. J. Rogers, and P. Kundur, "A fundamental study of inter-area oscillations in power systems," *IEEE Trans. Power Syst.*, vol. 6, no. 3, pp. 914–921, Aug. 1991.
[54] M. Pai, *Energy Function Analysis for Power System Stability*. Boston, MA, USA: Springer, 2012.
[55] P. J. Rousseeuw, "Silhouettes: A graphical aid to the interpretation and validation of cluster analysis," *J. Comput. Appl. Math.*, vol. 20, no. 1, pp. 53–65, 1987.

MEHDI BABAEI received the B.Sc. degree in electrical power engineering from the Sharif University of Technology (SUT), Tehran, Iran, in 2005, and the M.Phil. degree in electrical power engineering from Curtin University, in 2017, where he is currently pursuing the Ph.D. degree. From 2005 to 2015, he was with Faraniroo Company, Tehran, Iran, as an Electrical Engineer. His research interests include high voltage switchgears, power system transients, and power system stability studies.

S. M. MUYEEN (S'03–M'08–SM'12) received the B.Sc.Eng. degree from the Rajshahi University of Engineering and Technology (RUET), Bangladesh, formerly known as the Rajshahi Institute of Technology, in 2000, and the M.Eng. and Ph.D. degrees from the Kitami Institute of Technology, Japan, in 2005 and 2008, respectively, all in electrical and electronic engineering. He is currently an Associate Professor with the Department of Electrical and Computer Engineering, Curtin University, Perth, Australia. His research interests include power system stability and control, electrical machine, FACTS, energy storage system (ESS), renewable energy, and HVDC system. He is a Fellow of Engineers Australia.

SYED ISLAM received the B.Sc. degree in electrical engineering from the Bangladesh University of Engineering and Technology, Bangladesh, in 1979, and the M.Sc. and Ph.D. degrees in electrical power engineering from the King Fahd University of Petroleum and Minerals, Dhahran, Saudi Arabia, in 1983 and 1988, respectively. He was the John Curtin Distinguished Professor in electrical power engineering and the Director of the Centre for Smart Grid and Sustainable Power Systems, Curtin University, Perth, WA, Australia. He was the Dean of the Faculty of Science and Engineering, Curtin University, from 2011 to 2018. He has been a Visiting Professor with the Shanghai University of Electrical Power and Xi'an Jiatong University, China. He is currently the Dean of the School of Science Engineering and Information Technology, Federation University, Australia. He has extensive experience in international collaboration in both education and research with institutes and researchers in China and other countries. He has published over 270 technical papers in his area of expertise. His research interests include condition monitoring of transformers, wind energy conversion, and smart power systems. He is a Fellow of the Engineers Australia and the IET, a Senior Member of IAS, PES, and DEIS, and a Chartered Engineer in U.K., and a Chartered Professional Engineer in Australia. He is also a member of the Steering Committee of the Australian Power Institute and the WA EESA Board. He received the Dean's Medallion for research with Curtin University, in 1999, the IEEE T Burke Haye's Faculty Recognition Award, in 2000, the Curtin University Inaugural Award for Research Development, in 2012, and the Sir John Madsen Medal, in 2011 and 2014, for the Best Electrical Engineering Paper in Australia. He has been a Keynote Speaker and an Invited Speaker at many international workshops and conferences. He was the Guest Editor-in-Chief of the IEEE TRANSACTIONS ON SUSTAINABLE ENERGY, Special Issue on Variable Power Generation Integration into Grid. He is a Founding Editor of the IEEE TRANSACTIONS ON SUSTAINABLE ENERGY and an Associate Editor of the *IET Renewable Power Generation*.